

Modelling Power Law Dependencies of Frequency Dependent AC Conductivity and Permittivity of Conductor-Relaxor Composites

C. R. BOWEN^{1,*}, A.C.E. DENT¹, D. P. ALMOND¹,
AND T. P. COMYN²

¹Materials Research Centre, Department of Mechanical Engineering, University of Bath, Bath, BA2 7AY, UK

²Institute for Materials Research, University of Leeds, Leeds, LS2 9JT, UK.

Porous lead magnesium niobate-lead titanate (PMN-PT 90:10) relaxors were impregnated with water to provide a model conductor-insulator mixture, to study their power law frequency dependency of ac conductivity, permittivity and phase angle. Relaxor materials with a range of open porosity filled with water created composites with conductor volume fractions ranging from 8.2% to 22.2%. The use of a high relative permittivity PMN-PT (~8000) enabled the power law dispersion to be observed at relatively low frequencies (~2 kHz). Good agreement was obtained between experimental data and predicted results based on a logarithmic mixing rule with a strong correlation between the power law exponent and conductor-insulator fraction. The model and numerical methods presented are considered a simple approach to interpret and predict and the frequency dependent properties of materials which similar heterogeneity.

1. Introduction

Heterogeneous materials that contain random distributions of conductive and insulating phases are present in a wide variety of materials, such as ceramics polymers and composites (including ferroelectrics). Many of these materials exhibit a similar frequency (f) dependent conductivity and permittivity, often termed Jonscher's "Universal Dielectric Response" (UDR) [1]. A characteristic of the UDR is that at low frequencies the bulk ac conductivity is frequency independent, $\sigma(0)$, but at higher frequencies the ac conductivity increases following a power law behaviour such that,

$$\sigma(\omega) = \sigma(0) + A\omega^n \quad (1)$$

where ω is angular frequency ($2\pi f$), A is a constant and $0 < n < 1.0$. The relative permittivity (ϵ) can also be expressed by a power-law decay [2] such that,

$$\epsilon \propto \omega^{n-1} \quad (2)$$

Previous work [3, 4] has shown that a large network of resistors (R) and capacitors (C) can be used to simulate the microstructure of a heterogeneous material which consists

Received September 1, 2007.

*Corresponding author. E-mail: c.r.bowen@bath.ac.uk

of a random distribution of conducting (resistors) and insulating regions (capacitors). The electrical networks exhibit fractional power law frequency dependences of permittivity and ac conductivity, which are remarkably similar to Eqns. 1 and 2. The main observations from the study of RC networks [3, 4, 5] were:

- (i) at low frequencies, where $R^{-1} > \omega C$, currents flow preferentially through the resistors
- (ii) at high frequencies, where $R^{-1} < \omega C$, currents flow preferentially through the capacitors
- (iii) at intermediate frequencies, where $R \sim \omega C$, currents flow through both types of component
- (iv) the power law dependencies of the electrical networks are observed in the frequency range where the ac conductivities of the resistors and capacitors are similar; i.e. at the condition $R \sim \omega C$
- (v) the power law response of the network is related to the resistor and capacitor values by a simple logarithmic mixing rule where the complex conductivity of the network ($\sigma^*_{\text{network}}$) could be described as, $\sigma^*_{\text{network}} = (i\omega C)^\alpha (R^{-1})^{1-\alpha}$, where α is the fraction of capacitors.

If a conductor-insulator composite material is modelled as a large network of conductive and insulating regions in which the aspect ratios of two phases are equal, the bulk ac conductivity and relative permittivity predicted by the logarithmic mixing rule are given by Equations 3 and 4 respectively [3, 4, 5].

$$\sigma_{\text{meas.}} = (\omega \varepsilon \varepsilon_0)^\alpha (\sigma)^{1-\alpha} \cos(\alpha\pi/2) \quad (3)$$

$$\varepsilon_{\text{meas.}} = (\omega \varepsilon_0)^{\alpha-1} \varepsilon^\alpha \sigma^{1-\alpha} \sin(\alpha\pi/2) \quad (4)$$

where σ is the conductivity of the conducting phase, ε is the relative permittivity of the insulating (dielectric) phase, ε_0 is the permittivity of free space and α is the fractional volume of the material occupied by the dielectric phase. Equations 3 and 4 predict that the power law exponent (n) in the UDR (Eqns. 1 and 2) is related to the fractional volumes of the conducting ($1-\alpha$) and insulating (α) regions in a material. The RC network approach and logarithmic mixing rule has been used to model the electrical characteristics of two-phase conductor-insulator composites, such as lead zirconate titanate (PZT)-water [6], PZT-conducting polymer composites [7] Co-ZrO₂ conducting films [8, 9], and water confined in molecular sieve material [10, 11]. It has also been used to understand the role of conductivity in enhancing the dielectric constant of holmium doped BaTiO₃ [12]. Jankowski used RC networks to model the permittivity and dielectric loss in NiZn ferrites [13].

At this stage it is necessary to consider the appropriate frequency range for studying the power law dispersions. For a two-phase material consisting of a conductor of conductivity σ and an insulator of relative permittivity ε , the power law frequency dependences of ac conductivity and permittivity are observed when $\sigma \sim \omega \varepsilon \varepsilon_0$ (equivalent to the condition $R \sim \omega C$). In previous work [6, 7, 14] since $\varepsilon = 1500$ for PZT and $\sigma \sim 0.1 \text{ S/m}$ for the water, the condition $\sigma \sim \omega \varepsilon \varepsilon_0$ is satisfied at $\sim 1.2 \text{ MHz}$. While measurements in this frequency range are possible using standard impedance spectroscopy methods, it is difficult to examine significantly higher frequencies by the same method. Since electrical characterisation can be readily undertaken from $\sim 0.1 \text{ Hz}$ to 1 MHz it would be advantageous to observe the power law dependencies in the $1\text{--}10 \text{ kHz}$ range since it would be possible to probe a range of frequencies where $\sigma \gg \omega \varepsilon \varepsilon_0$, $\sigma \sim \omega \varepsilon \varepsilon_0$ and $\sigma \ll \omega \varepsilon \varepsilon_0$. One method of ‘tuning’ the electrical response to observe power law behaviour at lower frequencies is to lower the magnitude of σ for the conductive material or increase ε for the insulating material.

A reduction of water conductivity is limited since its conductivity is dominated by ions which leach into water when in contact with the ionically bonded ceramic. Therefore, an increase in the permittivity of the ceramic was sought.

In this work, lead magnesium niobate- lead titanate (PMN-PT) relaxor ferroelectric ceramics with open porosity were used as the insulating material of high permittivity. The open porosity volume fraction within the PMN-PT was infiltrated with water (a conductor) to create a model conductor-insulator composite. The advantage of this approach is the ease at which the conductivity of the water (σ_{water}) and relative permittivity of the relaxor ($\epsilon_{\text{relaxor}}$) can be individually determined. The formation of the relaxor-water composites is also relatively simple. Since water is expected to infiltrate the open porosity of the relaxor, the fraction of conductor ($1-\alpha$) in Eqns. 3 and 4 is related to the open porosity volume fraction (Π), such that

$$1 - \alpha = \Pi \quad (5)$$

Due to the high relative permittivity of the PMN-PT (~ 8000) the power law dependencies are expected to be observed at relatively low frequencies. A range of open porosity fractions were manufactured to examine the influence of conductor-insulator volume fraction on frequency dependent ac conductivity and permittivity and also evaluate the applicability of the logarithmic mixing rule. The correlation between power law exponent (n) of the UDR (Eqns.1 and 2) and the conductor-insulator fraction will be examined. Both experimental and model predictions are presented.

2. Experimental

2.1 Material Manufacture

The insulator material chosen for this study was 0.9 ($\text{PbMg}_{1/3}\text{Nb}_{2/3}\text{O}_3$) – 0.1 (PbTiO_3), which is a relaxor ferroelectric with a transition temperature (T_C) of approximately 40°C. The powders were manufactured via the columbite route by calcining PbO and TiO_2 (Aldrich) with pre-reacted MgNb_2O_6 (HC Starck) at 800°C for 2 hours. The powders were processed in a high speed attrition mill both prior to and after calcination, providing a single phase material (as determined by x-ray diffraction) with a particle size, d_{50} , of ca. 200 nm. To create open and interconnected porosity, polyethylene oxide (PEO) particles were added to the powder in various mass fractions (0wt.%, 3wt.%, 5wt.% and 7wt.%). The PEO was added to the powder and dry-milled for 1 hour without the use of media. Green pressed pellets were formed using a uni-axial press with a pressure of 100 MPa. The PEO was burnt out after pellet formation by heating slowly to 500°C at 10°C per hour. The pellets were subsequently sintered at 1000°C for 2 hours in a box-furnace, and ground to provide parallel surfaces prior to characterisation.

2.2 Density Measurement

For the porous relaxor materials it was necessary to determine density and establish the volume fraction of interconnected open porosity (Π), which would control the fraction of the conductive phase (water). The European standard EN623-2:1993 was followed using the hydrostatic weighing technique. This requires the masses of the dry ceramic, the ceramic impregnated with water and the impregnated ceramic weighed in water. The procedures used for drying and water infiltration were consistently used for each sample and also applied

when preparing the PMN-PT water composites for electrical measurement. All water used throughout the handling of the materials was reagent grade distilled water (Fisher Scientific) and attention was paid to avoid any contamination. Samples were submerged in water and placed in a vacuum chamber to remove gases and infiltrate the pores. The vacuum was cycled up to ~ 1.5 bar reverse gauge pressure and held for ~ 1 hour before returning to atmospheric. This cycle was repeated until no more out gassing was visible for at least 15 minutes. This typically took 24 hours. After removal from the vacuum the samples had noticeably been refrigerated by the expansion of the gases, so were left to condition at room temperature for 2 hours. The wet mass measurements were made on an analytical balance (Sartorius) with an accuracy ± 0.1 mg. Samples were cleaned with ethanol before drying at $100 \pm 5^\circ\text{C}$ for 24 hours and cooled inside a desiccator to room temperature for a further 24 hours. The dry mass was determined and used to calculate density and porosity, based on the theoretical density of 90:10 PMN-PT (8.14g cm^{-3}) [15].

2.3 Electrical Measurements

Electrodes were formed on the dry relaxor ceramic using silver paint (RS Products). The materials were characterised from a frequency of 0.1 Hz to 1 MHz at a voltage of $1V_{\text{rms}}$, using a Solartron 1260 Impedance Analyser with bespoke test fixtures and a 1296 Dielectric Interface. All electrical measurements were made under controlled temperature conditions ($22 \pm 1^\circ\text{C}$), to avoid temperature effects due to the low T_c of the relaxor (40°C).

To evaluate the properties of the relaxor-water composites the porous relaxor materials were vacuum infiltrated with water, following the method previously described for density measurements. Water impregnated samples were removed from the water, any surface liquid removed with lint free cloth, and then rapidly tested to avoid dehydration of the water which would affect the relative fraction of conductive material.

To evaluate the electrical properties of the conducting water phase (σ_{water}), the water used for sample immersion was retained to ensure that the water tested was representative of the water within the ceramic pore space. Six measurements were made and an average taken.

For the samples tested, the ac conductivity was calculated from the impedance data using Eqn. 6,

$$\sigma = \frac{Z'}{Z'^2 + Z''^2} \cdot \frac{t}{A} \quad (6)$$

where Z' and Z'' are the real and imaginary parts of the impedance, A is the area of the sample and t is the sample thickness. The relative permittivity was calculated for the impedance data using Eqn. 7,

$$\varepsilon = -\frac{Z''}{Z'^2 + Z''^2} \cdot \frac{t}{\varepsilon_0 \omega \cdot A} \quad (7)$$

3. Results and Discussion

3.1 Density Measurements

Figure 1a shows the decrease in bulk density of the relaxor ceramic with increasing weight fraction of polymer additive. The increase in open porosity volume fraction with decrease

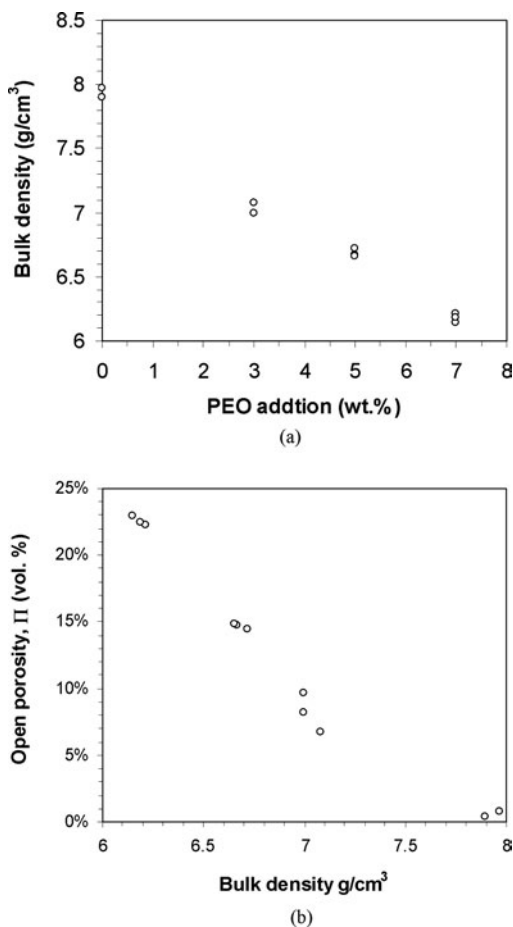
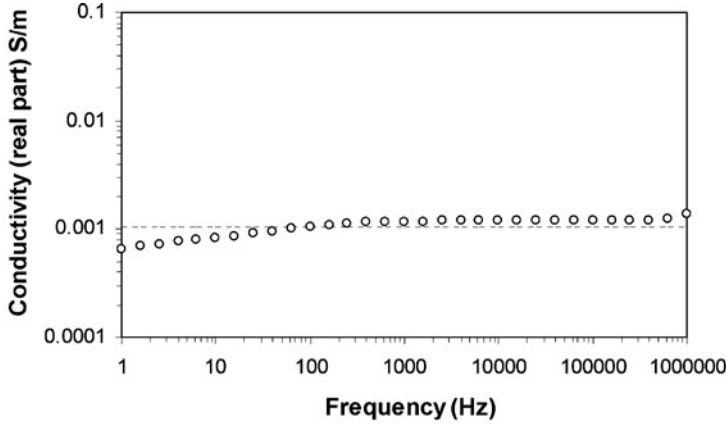


Figure 1. Variation of (a) bulk density with polymer addition (b) open porosity with bulk density.

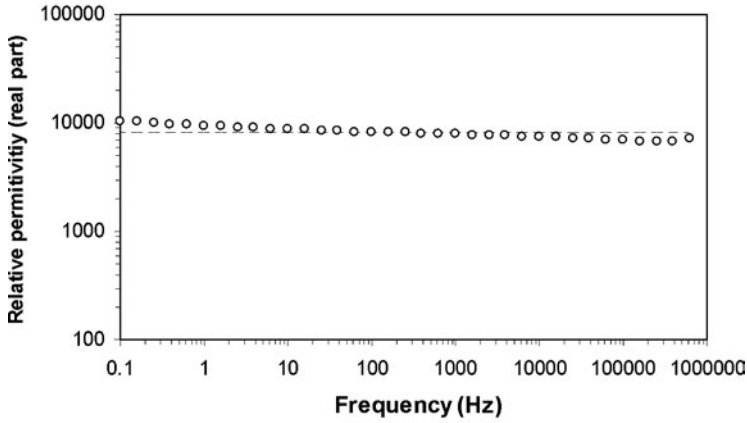
in bulk density is shown in Figure 1b. Since water is assumed to enter only open porosity, the magnitude of the open porosity is used to estimate the conductor volume fraction (Π) in the relaxor-water composites. While all samples were impregnated with water and tested, this paper presents data on a representative sample from each of the volume fractions. This corresponds to samples with Π values of 8.2%, 14.8% and 22.2%. A dense material, with no polymer addition and a small open porosity volume fraction of 0.4%, was also tested to determine the properties of the relaxor material ($\epsilon_{\text{relaxor}}$).

3.2 Water Conductivity (σ_{water}) and Dense Relaxor Permittivity ($\epsilon_{\text{relaxor}}$)

Figure 2a shows the real part of conductivity of the water, which had been retained after immersion in the relaxor ceramic so that it is representative of the water in the pore space. Figure 2b shows the relative permittivity for the dense relaxor material. Both are relatively featureless across the frequency range examined. The fall in water conductivity at low frequency is likely to be due to electrode polarisation [6]. The mean value of conductivity and relative permittivity for each phase was at 100 Hz and was considered as being representative of each material. This resulted in a water conductivity of $\sigma_{\text{water}} = 1 \times 10^{-3}$ S/m and a relative



(a)



(b)

Figure 2. (a) real part of conductivity of water (b) real part of permittivity of dense material (0.4% open porosity). Dotted line is value taken at 100 Hz.

permittivity of the PMN-PT of $\epsilon_{\text{relaxor}} = 8250$ (see dotted lines in Fig. 2a,b). Based on these measurements the condition $\sigma_{\text{water}} \sim \omega \epsilon_{\text{relaxor}} \epsilon_0$ is attained at a frequency of ~ 2.5 kHz.

3.3 AC Conductivity of Relaxor-Water Composites

The ac conductivity of the porous PMN-PT samples with open porosity volume fractions of 8.2, 14.8 and 22.2% saturated with water are shown in Figure 3. The ac conductivities of the relaxor-water composites exhibit a frequency dispersion that is qualitatively similar to the UDR (Eqn. 1). The measured water conductivity (σ_{water}), dense ceramic permittivity ($\epsilon_{\text{relaxor}}$) and the volume fraction of water within open pores (Π) were used to calculate the frequency dependent component of the ac conductivity (Eqn. 3), which was added to the low frequency percolation plateau, $\sigma(0)$, as in Eqn. 8 [6].

$$\sigma_{\text{composite}} = \sigma(0) + (\omega \epsilon_{\text{relaxor}} \epsilon_0)^{1-\Pi} (\sigma_{\text{water}})^\Pi \cos((1 - \Pi)\pi/2) \quad (8)$$

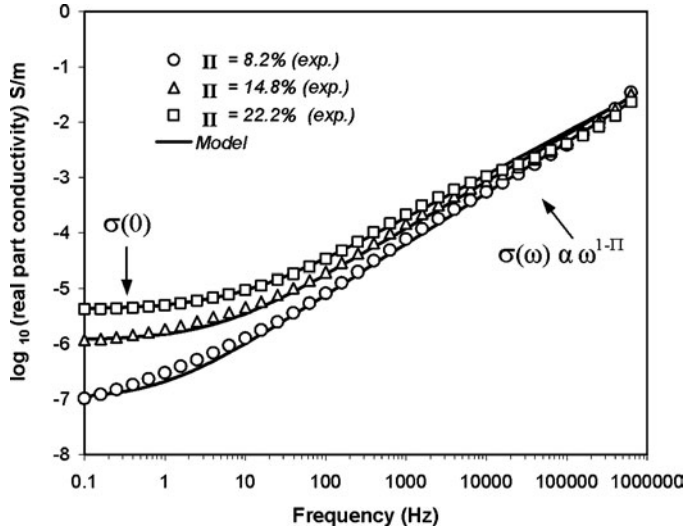


Figure 3. Real part of conductivity versus frequency for water impregnated relaxor materials. Experimental and model predictions (Eqn. 8) shown. For model $\sigma_{\text{water}} = 1 \times 10^{-3}$ S/m, $\epsilon_{\text{relaxor}} = 8250$ and Π is the open porosity volume fraction (8.2%, 14.8% and 22.2%).

Eqn. 8 predicts that the power law region is related to the fraction of insulating ceramic ($1-\Pi$) and $\sigma \propto A\omega^{1-\Pi}$ (i.e. $n = 1-\Pi$ in Eqn. 1). There is good agreement with the experimental data (data points) and model prediction (solid lines) in Figure 3; with the slope of the power law region (n) decreasing as porosity is increased and the fraction of ceramic is reduced (as predicted by Eqn. 8). In the low frequency region where $\sigma_{\text{water}} \gg \omega\epsilon_{\text{relaxor}}\epsilon_0$ currents are expected to flow through the percolated water phase within the open porosity. This explains the increase in the magnitude of the frequency independent region, $\sigma(0)$, as the level of open porosity (and the volume fraction of water) in the composite is increased from 8.2% to 22.2%.

3.4 Phase Angle of Relaxor-Water Composites

The phase angle (θ) between current and voltage was determined from Eqn. 9.

$$\theta = \tan^{-1}(Z''/Z') \quad (9)$$

Figure 4 shows the frequency dependence of the phase angle of the relaxor ceramics with open porosity levels of 8.2, 14.8 and 22.2vol.% saturated with water along with data for the dense material which had also been immersed in water. For the dense material (0.4% open porosity) the phase angle remains $\sim 90^\circ$ for all frequencies and the insulating material is behaving in a capacitive manner. For the water impregnated samples with higher porosities a different behaviour is observed. At low frequencies (< 10 Hz) where $\sigma_{\text{water}} > \omega\epsilon_0\epsilon_{\text{relaxor}}$ the phase approaches 0° since the currents are flowing exclusively through the water in the interconnected and open pores. This is particularly true for the high porosity ceramics. At intermediate frequencies ($\sim 100\text{--}3000$ Hz) where $\sigma_{\text{water}} \sim \omega\epsilon_0\epsilon_{\text{relaxor}}$ currents are flowing through both water and ceramic and the phase angle is relatively frequency independent. The logarithmic mixing rule (Eqn. 8) predicts that in regions where $\sigma_{\text{water}} \sim \omega\epsilon_0\epsilon_{\text{relaxor}}$ the

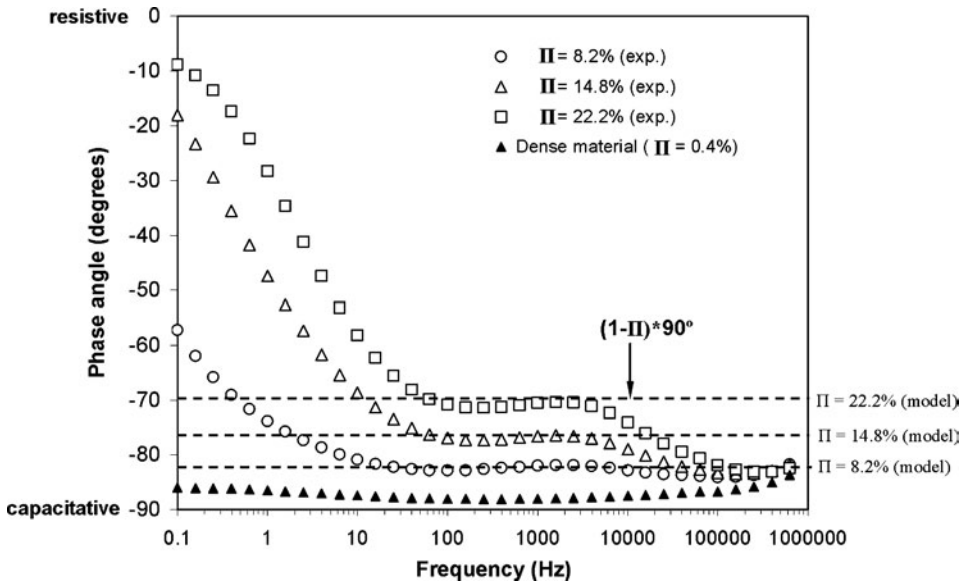


Figure 4. Phase angle versus frequency for water impregnated relaxor materials. Experimental data shown as data points. Predicted phase angle $(1-\Pi)*90^\circ$ (Eqn. 8) shown as a dotted line for comparison.

phase angle $\theta = [(1-\Pi).\pi/2]$ radians. The dotted lines in Figure 4 are the predicted phase angles with good agreement with the experimental data for the water impregnated porous materials. Such a response is also in good agreement with RC network simulations of phase angle, for example see data in [3, 4, 16]. At higher frequencies where $\sigma_{\text{water}} < \omega\epsilon_0\epsilon_{\text{relaxor}}$ the ac currents are expected to flow exclusively through the percolated insulating ceramic and the composite should behave in a capacitive manner. The experimental data shows that at frequencies >10 kHz the phase angle does indeed increase and approach 90° .

3.5 Relative Permittivity of Relaxor-Water Composites

Figure 5 shows the relative permittivity as a function of frequency for the relaxors with open porosity levels of 8.2, 14.8 and 22.2% saturated with water. The water conductivity (σ_{water}), dense ceramic relative permittivity ($\epsilon_{\text{relaxor}}$) and the volume fraction of water (Π), were used to calculate the frequency dependent component of the real part of permittivity, Eqn. 10.

$$\epsilon_{\text{composite}} = (\omega\epsilon_0)^{-\Pi} \epsilon_{\text{relaxor}}^{1-\Pi} \sigma_{\text{water}}^\Pi \sin((1 - \Pi)\pi/2) \tag{10}$$

The equation predicts that the gradient of the power law dispersion to be equal to $-\Pi$ where $\epsilon_{\text{composite}} \propto \omega^{-\Pi}$. Figure 5 shows good agreement between experimental (data points) and predicted results (solid lines), in particular the slope of the power law dispersions. In some cases the predicted permittivity is smaller than the experimental data. At high frequencies (>100 kHz) the frequency dependent permittivity begins to flatten out. In this frequency region the magnitude of the frequency dependent component of permittivity based on Eqn. 10 becomes relatively small and the experimental data deviates from predicted response. In this frequency range alternating currents are flowing exclusively through the ceramic regions and the phase angle approaches 90° (see Figure 4); leading to a frequency independent permittivity which approaches that of the porous PMN-PT material.

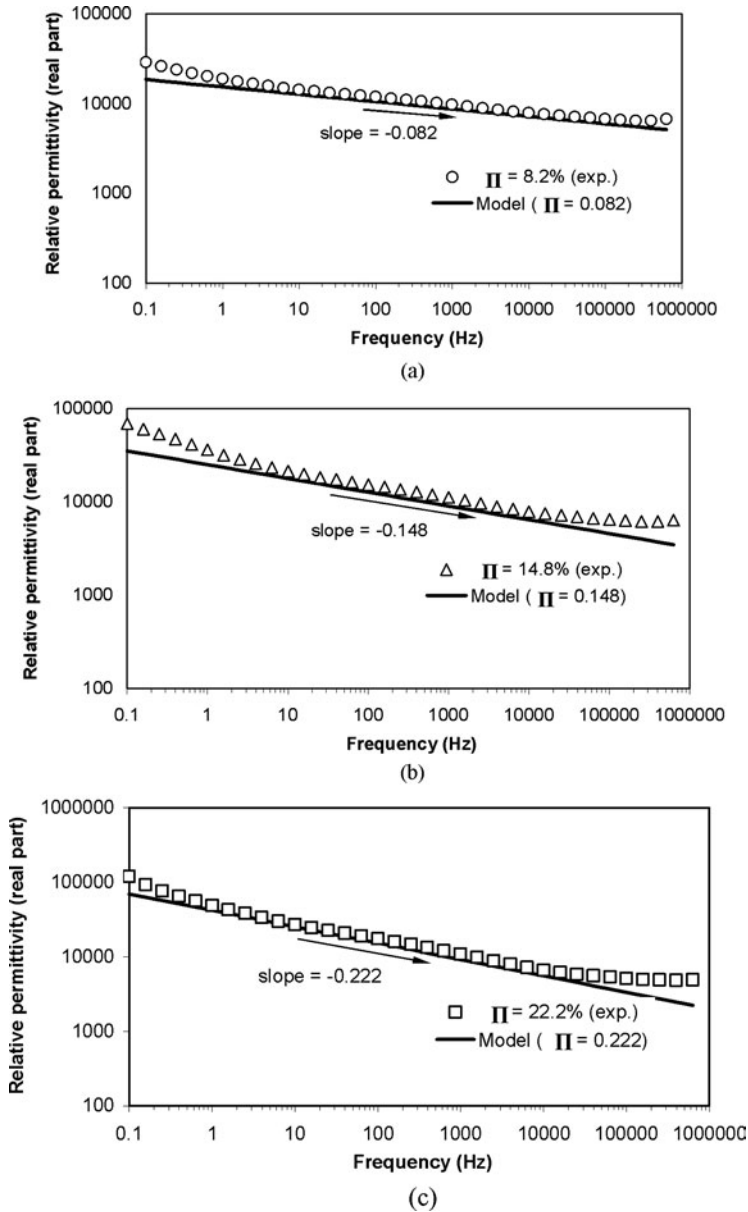


Figure 5. Real part of permittivity versus frequency for water impregnated relaxor materials. Experimental and model predictions (Eqn. 10) shown. For model $\sigma_{\text{water}} = 1 \times 10^{-3}$ S/m, $\epsilon_{\text{relaxor}} = 8250$ and Π is the open porosity volume fraction (8.2%, 14.8% and 22.2%).

4. Conclusions

The work has used PMN-PT relaxor-water composites as a model system to evaluate the applicability of simple logarithmic mixing rules to predict the frequency dependent ac conductivity, permittivity and phase angle of conductor-insulator composites. A range of porous relaxor materials where impregnated with water to create composites with a range of conductor volume fraction (8.2% to 22.2%). Due to the high relative permittivity of the

PMN-PT (~ 8000) the power law dependencies were observed at relatively low frequencies since the condition $\sigma_{\text{water}} \sim \omega \varepsilon_0 \varepsilon_{\text{relaxor}}$ is satisfied at ~ 2 kHz. Good agreement was obtained between experimental data and predicted results revealing a strong correlation between the power law exponent (n) of the UDR and the volume fraction of conductor (Π) and insulator ($1-\Pi$) in the composite. The use of RC networks and the logarithmic mixing rule is a simple, yet effective, approach for the prediction and interpretation of the frequency dependent properties (ac conductivity, permittivity and phase angle) of heterogeneous materials that can be considered as a microstructural network of conducting and insulation components.

Acknowledgments

The authors gratefully acknowledge the UK Great Western Research (GWR) and Bath Institute for Complex Systems (BICS) for supporting this research.

References

1. A. K. Jonscher, The 'universal' dielectric response, *Nature*. **267**, 673 (1977).
2. C. Brosseau, P. Quéffelec, and P. Talbot, Microwave characterization of filled polymers. *J. App. Phys.* **89**, 4532–4540 (2001).
3. D. P. Almond and B. Vainas, The dielectric properties of random R–C networks as an explanation of the 'universal' power law dielectric response of solids. *J. Phys. Condens. Matter* **11**, 9081 (1999).
4. B. Vainas, D. P. Almond, J. Luo, and R. Stevens, An evaluation of random R-C networks for modelling the bulk ac electrical response of ionic conductor. *Solid State Ionics* **126**, 65 (1999).
5. K. Lichtenecker, Die dielektrizitätskonstante natürlicher und künstlicher mischkörper. *Z. Phys.* **27**, 115 (1926).
6. D. P. Almond and C. R. Bowen, Anomalous power law dispersions in ac conductivity and permittivity shown to be characteristic of microstructural electrical networks. *Phys. Rev. Lett.* **92**, 157601–1 (2004).
7. D. P. Almond, C. R. Bowen, and D. A. S. Rees, Composite dielectrics and conductors: simulation, characterisation and design. *J. Phys. D: Appl. Phys.* **39**, 1295–1304 (2006).
8. B. J. Hattink, A. Labarta, M. García del Muro, X. Batlle, F. Sánchez, and M. Varela, Competing tunneling and capacitive paths in Co-ZrO₂ granular thin films. *Phys. Rev. B* **67**, 033402 (2003).
9. Z. Konstantinović, M. García del Muro, X. Batlle, A. Labarta, and M. Varela, Nanostructural origin of the ac conductance in dielectric granular metals: The case study of Co₂₀(ZrO₂)₈₀. *App. Phys. Lett.* **91**, 052108 (2007).
10. M. Kinka, J. Banys, J. Macutkevicius, and A. Meskauskas, Conductivity of nanostructured mesoporous MCM-41 molecular sieve materials. *Electrochimic Acta* **51**, 6203–6206 (2006).
11. M. Kinka, J. Banys, J. Macutkevicius, A. Pöppel, W. Böhlmann, V. Umamaheswari, M. Hartmann, and G. Völkel, Dielectric response of water confined in MCM-41 molecular sieve material. *Phys. Stat. Sol. (b)* **242**, R100–R102 (2005).
12. F. Chang, T. Li, Y. Ge, Z. Chen, Z. Liu, and X. Jing, Electrical properties and positron annihilation study of (Ba_{1-x}Ho_x)TiO₃ ceramics **42**, 7109–7115 (2007).
13. S. Jankowski, Dielectric dispersion in polycrystalline ferrites: Random network model. *J. Am. Ceram. Soc.* **71**, C176 (1988).
14. C. R. Bowen, and D. P. Almond, Modelling the 'universal' dielectric response in heterogeneous materials using microstructural electrical networks, *Materials Science and Technology* **22**, 719–724 (2006).
15. T. Ando, R. Suyama, and K. Tanemoto, Preparation of Pb(Mg_{1/3}Nb_{2/3})O₃-PbTiO₃ powder by a wet chemical process, *Jap. J. App. Phys.* **30**, 775–779 (1991).
16. B. Vainas, Modelling the 0.6–0.7 power law of permittivity and admittance frequency responses in random R-C networks, arXiv:cond-mat/0508170v2